JOURNAL OF AIRCRAFT
Vol. 44, No. 2, March–April 2007

Thin-Airfoil Theoretical Interpretation for Gurney Flap Lift Enhancement

Tianshu Liu* and J. Montefort†
Western Michigan University, Kalamazoo, Michigan 29008

DOI: 10.2514/1.27680

Thin-airfoil theory is applied to the lift problem of an airfoil with a Gurney flap. The lift and pitching moment coefficient increments are given as a square-root function of the relative Gurney flap height, and they are proportionally related. This model interprets the Gurney flap lift enhancement as a special camber effect. The theoretical relations are in good agreement with experimental and numerical data for several different wings. The theoretical method developed in this paper can be applied to similar trailing-edge devices for lift enhancement, and it is useful in the preliminary design of these flow control devices.

Nomenclature

A_n	=	Fourier coefficients for $\gamma(x)$
C_l	=	sectional lift coefficient
$C_{m,c/4}$	=	pitching moment coefficient relative to $c/4$
c	=	main element chord length
c'	=	total projected chord length on x coordinate, $c + l\cos\delta$
L'	=	sectional lift
l	=	deflected segment length
$\boldsymbol{m}$	=	unit induced velocity vector
$\boldsymbol{n}$	=	unit normal vector on camber line
s	=	arc length along camber line
V_∞	=	freestream velocity
x	=	coordinate along main element
y	=	coordinate normal to main element or camber line, $y = f(x)$
y_A	=	vertical length scale
α	=	angle of attack
$\gamma(x)$	=	strength of vortex sheet
ΔC_l	=	change of lift coefficient
$\Delta C_{m,c/4}$	=	change of pitching moment coefficient
δ	=	effective hydrodynamic deflection angle
ε	=	small parameter, $(l/c)\cos\delta$
η	=	nondimensional coordinate, y/y_A
θ	=	angular variable in thin-airfoil theory
θ_c	=	angular variable corresponding to breaking point $x = c$
ξ	=	nondimensional coordinate, x/c

Introduction

THE Gurney flap is a short strip installed along the trailing edge on the pressure surface perpendicular to the chord line of a wing. The Gurney flap, which was first used by the race-car driver Dan Gurney, was introduced by Liebeck [1] to the aeronautical community, and considerable measurements and calculations have been performed to determine the aerodynamic characteristics of wings with Gurney flaps [2–10]. Generally speaking, Gurney flaps can increase the lift at a cost of increasing the drag. There are few in-depth analytical studies on the physical mechanism of the Gurney flap lift enhancement, although it is often conceptually attributed to the modification of the trailing-edge Kutta condition. Imposing a finite pressure difference at the trailing edge in a panel method, Jeffrey et al. [4] were able to mimic an increase of aerodynamic loading generated by Gurney flaps. By numerically solving the Reynolds averaged Navier-Stokes equations, Jang et al. [7] predicted the shift of the lift curve as a function of the relative Gurney flap height. The effect of a Gurney flap can also be modeled by adding a vortex at the trailing edge that turns the flow downward and generates additional lift as a result. However, the intuitive, analogous approach cannot directly reveal the relationship between the lift enhancement and geometrical parameters such as the Gurney flap height.

The objective of this work is to explore the physical mechanism of the Gurney flap lift enhancement and seek the analytical relation between the lift enhancement and relative Gurney flap height based on thin-airfoil theory. The formulation of thin-airfoil theory is generalized for Gurney flaps because the conventional assumption of small camber line slope in the classical thin-airfoil theory is not applicable. The increments in the lift and pitching moment coefficients by a Gurney flap are derived and compared with the experimental and computational results. The proposed methodology is applicable to similar trailing-edge devices for flow control.

Thin-Airfoil Theory for Gurney Flap

Thin-airfoil theory is originally formulated based on an assumption that the camber line slope of an airfoil is small [11,12]. The formulation given in most aerodynamics textbooks cannot be directly applied to Gurney flaps that are installed perpendicularly to the main airfoil. Here, we derive a thin-airfoil integral equation applicable to Gurney flaps. Figure 1 shows a camber line given by $y = f(x)$, its unit normal vector, small vortex segment ds, and the corresponding unit induced velocity vector. For the camber line to be a streamline, the total normal velocity on the camber line should vanish. This leads to the general thin-airfoil integral equation for the strength $\gamma(x)$ of the vortex sheet

$$\boldsymbol{n}\cdot V_\infty + \boldsymbol{n}\cdot\int_a^b \frac{\boldsymbol{m}\gamma(s)}{2\pi r}\,\mathrm{d}s = 0 \tag{1}$$

where

$$\boldsymbol{n} = \frac{1}{\sqrt{1+(dy/dx)^2}}\left(-\frac{dy}{dx}\boldsymbol{i} + \boldsymbol{j}\right)$$

$$\boldsymbol{m} = r^{-1}[(y-y_s)\boldsymbol{i} - (x-x_s)\boldsymbol{j}] \qquad r = \sqrt{(x-x_s)^2 + (y-y_s)^2}$$

We define the angle between the freestream velocity and unit vector $\boldsymbol{i}$ along x coordinate as the angle of attack. At this stage, the coordinate

Received 6 September 2006; revision received 30 November 2006; accepted for publication 30 November 2006.

*Corresponding Author, Associate Professor, Department of Mechanical and Aeronautical Engineering, G-220, Parkview Campus, Kalamazoo, MI 49008; tianshu.liu@wmich.edu. Member AIAA.

†Assistant Professor, Department of Mechanical and Aeronautical Engineering, Parkview Campus, Kalamazoo, MI 49008

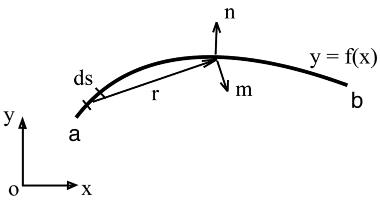

Fig. 1 Camber line, normal vector, and induced velocity vector.

system (x, y) defined by the unit vectors $\boldsymbol{i}$ and $\boldsymbol{j}$ is arbitrary. Conventionally, the origin of the coordinate system is located at the leading edge and the x axis is defined along the chord line for a single-element airfoil. For Gurney flaps, the x axis is on the chord line of the main element of the airfoil. Further, Eq. (1) becomes

$$V_\infty\left(\sin\alpha - \frac{dy}{dx}\cos\alpha\right) = \frac{dy}{dx}\int_a^b \frac{(y-y_s)\gamma(s)}{2\pi r^2}\,\mathrm{d}s + \int_a^b \frac{(x-x_s)\gamma(s)}{2\pi r^2}\,\mathrm{d}s \tag{2}$$

For a thin airfoil, the chord length is usually much larger than the vertical length scale. After substituting the nondimensional variables into Eq. (2) and neglecting the smaller terms of the order of $(y_A/c)^2$, Eq. (2) is approximated by

$$V_\infty\left(\sin\alpha - \frac{dy}{dx}\cos\alpha\right) = \frac{dy}{dx}\int_a^b \frac{(y-y_s)\gamma(s)}{2\pi(x-x_s)^2}\,\mathrm{d}s + \int_a^b \frac{\gamma(s)}{2\pi(x-x_s)}\,\mathrm{d}s \tag{3}$$

It is emphasized that the assumption $(y_A/c)^2 \ll 1$ does not mean that the local slope dy/dx is small. Gurney flap is just a typical case where $(y_A/c)^2$ is small, but dy/dx is locally large. The first term in the right-hand side of Eq. (3) cannot be neglected for Gurney flaps because dy/dx is no longer small. In the special case where $dy/dx \ll 1$ and $\alpha \ll 1$, Eq. (3) naturally reduces to the classical thin-airfoil integral equation.

To develop the thin-airfoil theory for Gurney flaps from Eq. (3), a simplified vortex model is proposed. As qualitatively illustrated in Fig. 2, a separation bubble forms immediately upstream of a Gurney flap, and two counter-rotating vortices (or alterative vortices) are generated behind the flap. This observation is supported by the computational fluid dynamics (CFD) simulation [7] and velocity measurement [4]. The separation bubble induced by the Gurney flap deflects the streamlines downward, resulting in the lift enhancement. The average angle between the main wing chord and deflected dividing streamline immediately upstream of the Gurney flap is denoted by δ. This is an effective hydrodynamic deflection angle depending on Reynolds number. The deflection angle is smaller than $\pi/2$.

Under the spirit of thin-airfoil theory, the lift problem of a Gurney flap is considered based on such a model for the effective camber line: a main vortex-sheet segment connected with a deflected short vortex-sheet segment, as shown in Fig. 3. It should be emphasized that the deflected vortex segment aerodynamically models the flow-deflecting effect by a Gurney flap, but not the Gurney flap itself. Therefore, the total projected chord on the x coordinate is $c' = c + l\cos\delta$. The camber line for a Gurney flap is given by $y = -\tan\delta(x-c)H(x-c)H(c'-x)$, where the Heaviside function is defined as $H(x) = 0$ for $x < 0$ and $H(x) = 1$ for $x \ge 0$. Thus,

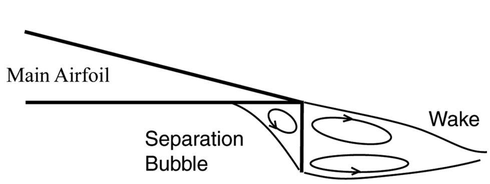

Fig. 2 Schematic of flowfield near a Gurney flap.

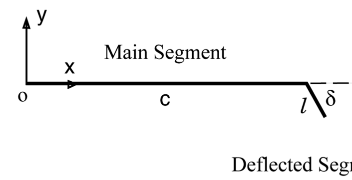

Fig. 3 Main and deflected vortex-sheet segments.

the slope of the camber line is $dy/dx = -\tan\delta H(x-c)H(c'-x)$. Furthermore, the differential arc length along the camber line is

$$\mathrm{d}s = \sqrt{1+(dy/dx)^2}dx = [1+(\tan\delta)^2H(x-c)H(c'-x)]^{1/2}dx \tag{4}$$

For $\alpha \ll 1$, substitution of the preceding relations into Eq. (3) yields

$$V_\infty[\alpha + K(x,\delta)] = \frac{K^2(x,\delta)}{\cos\delta}\int_c^{c'} \frac{\gamma(x_s)}{2\pi(x-x_s)}\,\mathrm{d}x_s + \int_0^{c'} \frac{\gamma(x_s)[1+K^2(x_s,\delta)]^{1/2}}{2\pi(x-x_s)}\,\mathrm{d}x_s \tag{5}$$

where $K(x,\delta) = 1 + (\tan\delta)^2H(x-c)H(c'-x)$. Equation (5) is the thin-airfoil integral equation for an airfoil with a Gurney flap. The terms containing $K(x,\delta)$ represent the effect of the Gurney flap on the main airfoil.

The first integral on the right-hand side of Eq. (5) makes this integral equation difficult to be solved directly. Further treatment of this integral is needed. The principal value of this improper integral is given by [13]

$$\int_c^{c'} \frac{\gamma(x_s)}{x-x_s}\,\mathrm{d}x_s = \int_c^{c'} \frac{\gamma(x_s)-\gamma(x)}{x-x_s}\,\mathrm{d}x_s + \gamma(x)\,\ell n\frac{x-c}{c'-x} \tag{6}$$

Introducing the nondimensional variable and a small parameter for Gurney flaps ($\varepsilon \ll 1$), we have an estimate

$$\int_c^{c'} \frac{\gamma(x_s)-\gamma(x)}{x-x_s}\,\mathrm{d}x_s = \int_1^{1+\varepsilon} \frac{\gamma(\xi_s)-\gamma(\xi)}{\xi-\xi_s}\,\mathrm{d}\xi_s \approx \gamma(\xi=1) = \gamma(x=c) \tag{7}$$

where the Kutta condition $\gamma(\xi = 1+\varepsilon) = 0$ is imposed. Based on this estimate, Eq. (5) can be formally written as

$$V_\infty\left(\alpha - \frac{K^2(x,\delta)}{V_\infty\cos\delta}g[\gamma(x),x] + K(x,\delta)\right) = \int_0^{c'} \frac{\gamma(x)[1+K^2(x,\delta)]^{1/2}}{2\pi(x-x_s)}\,\mathrm{d}x_s \tag{8}$$

where $g[\gamma(x), x]$ is defined as

$$g[\gamma(x),x] = \gamma(x)\,\ell n\frac{x-c}{c'-x} + \gamma(c) \tag{9}$$

Equation (8) has the same form as the classical thin-airfoil equation. When $g[\gamma(x), x]$ is treated as a known function, using the Glauert's method of Fourier series, we have

$$\gamma(\theta) = 2V_\infty[1+K^2(x,\delta)]^{-1/2}\left(A_0\frac{1+\cos\theta}{\sin\theta} + \sum_{n=1}^{\infty}A_n\sin n\theta\right) \tag{10}$$

where

$$A_0 = \alpha + \frac{\tan\delta(\pi-\theta_c)}{\pi} - \frac{(\tan\delta)^2}{\pi V_\infty\cos\delta}\int_{\theta_c}^{\pi} g[\gamma(x),x]\mathrm{d}\theta \tag{11}$$

$$A_n = \frac{2\tan\delta\sin(n\theta_c)}{\pi n} + \frac{2(\tan\delta)^2}{\pi V_\infty\cos\delta}\int_{\theta_c}^{\pi} g[\gamma(x),x]\cos(n\theta)\mathrm{d}\theta \tag{12}$$

The angular variable is related to x by $x = (c'/2)(1 - \cos\theta)$. The angle $\theta_c = \cos^{-1}[(\varepsilon - 1)/(\varepsilon + 1)]$ corresponds to the breaking point $x = c$ between the main element and Gurney flap. Substitution of Eqs. (11) and (12) yields a formal solution

$$\gamma(\theta) = \gamma_0(\theta) + C(\theta, \delta)\left(-\frac{1 + \cos\theta}{\sin\theta}\int_{\theta_c}^{\pi} g[\gamma(\theta'), \theta']\mathrm{d}\theta' + 2\sum_{n=1}^{\infty}\sin(n\theta)\int_{\theta_c}^{\pi} g[\gamma(\theta'), \theta']\cos(n\theta')d\theta'\right) \tag{13}$$

where

$$\gamma_0(\theta) = 2V_\infty[1 + K^2(x, \delta)]^{-1/2}\left[\left(\alpha + \frac{\tan\delta(\pi - \theta_c)}{\pi}\right)\frac{1 + \cos\theta}{\sin\theta} + \frac{2\tan\delta}{\pi}\sum_{n=1}^{\infty}\frac{\sin(n\theta)\sin(n\theta_c)}{n}\right] \tag{14}$$

and

$$C(\theta, \delta) = \frac{2(\tan\delta)^2}{\pi\cos\delta}[1 + K^2(x, \delta)]^{-1/2} \tag{15}$$

In fact, Eq. (13) is an integral equation of Fredholm type that is converted from Eq. (5). The fixed-point form of Eq. (13) is advantageous and it can be readily solved using Picard's method of successive approximations, that is,

$$\gamma^{(n+1)}(\theta) = \gamma_0(\theta) + C(\theta, \delta)\left[-\frac{1 + \cos\theta}{\sin\theta}\int_{\theta_c}^{\pi} g[\gamma^{(n)}(\theta'), \theta']d\theta' + 2\sum_{n=1}^{\infty}\sin(n\theta)\int_{\theta_c}^{\pi} g[\gamma^{(n)}(\theta'), \theta']\cos(n\theta')d\theta'\right] \tag{16}$$

where the initial solution is $\gamma^{(0)}(\theta) = \gamma_0(\theta)$. When the successive approximations converge in certain conditions, we have $\gamma(\theta) = \gamma^{(\infty)}(\theta)$. At this stage, the vortex-sheet strength for an airfoil with a Gurney flap has been obtained under the assumptions $(y_A/c)^2 \ll 1, \alpha \ll 1$, and $\varepsilon \ll 1$.

Lift Enhancement and Pitching Moment Change

As long as the vortex-sheet strength is determined, the lift and pitching moment can be calculated. The sectional lift is

$$L' = \rho_\infty V_\infty \int_0^{c'} \gamma(x)\mathrm{d}x = \rho_\infty V_\infty^2 c'\{Q(\theta_c) - Q(0) + [Q(\pi) - Q(\theta_c)][1 + (\tan\delta)^2]^{-1/2}\} \tag{17}$$

where the function $Q(\theta)$ is defined as

$$Q(\theta) = A_0(\theta + \sin\theta) + A_1\left(\frac{\theta}{2} - \frac{1}{4}\sin 2\theta\right) + \sum_{n=2}^{\infty}A_n\left(\frac{\sin(n-1)\theta}{2(n-1)} - \frac{\sin(n+1)\theta}{2(n+1)}\right) \tag{18}$$

Further, the sectional lift coefficient based on the chord of the main element is

$$C_l = \frac{L'}{\rho_\infty V_\infty^2 c/2} = 2(1 + \varepsilon)\left\{Q(\theta_c) + \left[A_0\pi + \frac{A_1\pi}{2} - Q(\theta_c)\right] \times [1 + (\tan\delta)^2]^{-1/2}\right\} \tag{19}$$

Similarly, the pitching moment coefficient relative to the leading edge is

$$C_{m,LE} = \frac{M_{LE}}{\rho_\infty V_\infty^2 c^2/2} = -(1 + \varepsilon)^2\{Q(\theta_c) - P(\theta_c) + [Q(\pi) - Q(\theta_c) - P(\pi) + P(\theta_c)][1 + (\tan\delta)^2]^{-1/2}\} \tag{20}$$

where the function $P(\theta)$ is defined as

$$P(\theta) = A_0\sin\theta + A_0\left(\frac{\theta}{2} + \frac{1}{4}\sin 2\theta\right) + \frac{A_2}{2}\left(\frac{\theta}{2} - \frac{1}{8}\sin 4\theta\right) + \frac{1}{2}\sum_{\substack{n=1\\n\neq 2}}^{\infty}A_n\left(\frac{\sin(n-2)\theta}{2(n-2)} - \frac{\sin(n+2)\theta}{2(n+2)}\right) \tag{21}$$

Because $\varepsilon \ll 1$ for Gurney flaps, using the following approximate relations $\theta_c \approx \cos^{-1}(\varepsilon - 1) \approx \pi - \sqrt{2\varepsilon}$, $\sin\theta_c \approx \sqrt{2\varepsilon}$, $\sin 2\theta_c \approx -2\sqrt{2\varepsilon}$, and $\sin 4\theta_c \approx -4\sqrt{2\varepsilon}$, we have $Q(\theta_c) \approx A_0\pi + A_1\pi/2$, and $P(\theta_c) \approx A_0\pi/2 + A_2\pi/4$. Note that the summation terms in Eqs. (18) and (21) are small for $\varepsilon \ll 1$ and thus they are neglected. Substitution of the preceding estimates into Eqs. (19) and (20) leads to the lift coefficient

$$C_l \approx \pi(2A_0 + A_1) \tag{22}$$

and the pitching moment coefficient relative to $c/4$

$$C_{m,c/4} \approx -\pi(A_1 - A_2)/4 \tag{23}$$

Interestingly, Eqs. (22) and (23) have the same forms as those in the classical thin-airfoil theory. The coefficients A_0, A_1, and A_2 can be further approximated for $\varepsilon \ll 1$. Therefore, the enhancement of the sectional lift coefficient by a Gurney flap is written as

$$\Delta C_l \approx C_l - C_{l,\text{base}} = \left(4\tan\delta + \frac{2(\tan\delta)^2}{V_\infty\cos\delta}(\bar{g}_1\cos\bar{\theta}_1 - \bar{g}_0)\right)\sqrt{2\varepsilon} \tag{24}$$

where $\bar{g}_0 = g[\gamma(\bar{\theta}_0), \bar{\theta}_0]$ and $\bar{g}_1 = g[\gamma(\bar{\theta}_1), \bar{\theta}_1]$ are the appropriate median values for $\bar{\theta}_0, \bar{\theta}_1 \in [\pi - \sqrt{2\varepsilon}, \pi]$. The change of the pitching moment coefficient produced by a Gurney flap is

$$\Delta C_{m,c/4} \approx -\left(\tan\delta - \frac{(\tan\delta)^2}{2V_\infty\cos\delta}(\bar{g}_2\cos 2\bar{\theta}_2 - \bar{g}_1\cos\bar{\theta}_1)\right)\sqrt{2\varepsilon} \tag{25}$$

where $\bar{g}_2 = g[\gamma(\bar{\theta}_2), \bar{\theta}_2]$ is the appropriate median value for $\bar{\theta}_2 \in [\pi - \sqrt{2\varepsilon}, \pi]$. Clearly, according to Eq. (24), the lift enhancement by a Gurney flap can be explained as a special camber effect. Furthermore, according to Eqs. (24) and (25), we know that $\Delta C_l/\Delta C_{m,c/4}$ is independent from the Gurney flap height. The initial approximation $\gamma^{(0)}(\theta) = \gamma_0(\theta)$ gives $\Delta C_l \approx 4\tan\delta\sqrt{2\varepsilon}$ and $\Delta C_{m,c/4} \approx -\tan\delta\sqrt{2\varepsilon}$. Thus, an initial but useful estimate for Gurney flaps is

$$\Delta C_l/\Delta C_{m,c/4} \approx -4 \tag{26}$$

Naturally, for $\varepsilon \ll 1$ and $\delta \ll 1$, the preceding relations are consistent with the classical thin-airfoil solution for a flapped airfoil [14,15].

Because the Gurney flap height is $h \propto l$ and the hydrodynamic deflection angle is Reynolds number dependent, according to Eq. (24), the Gurney flap lift enhancement for an airfoil is generally given by a square-root law

$$\Delta C_l = q(Re)\sqrt{h/c} \tag{27}$$

The same argument leads to the pitching moment change by a Gurney flap

$$\Delta C_{m,c/4} = -m(Re)\sqrt{h/c} \tag{28}$$

The negative sign indicates the nose-down moment generated by a Gurney flap. Because the hydrodynamic deflection angle is not known a priori and it is a free parameter, the present thin-airfoil theory only provides the functional relations. Nevertheless, the value of this theoretical model is that the intrinsic connection between the lift enhancement or pitching moment change and the Gurney flap

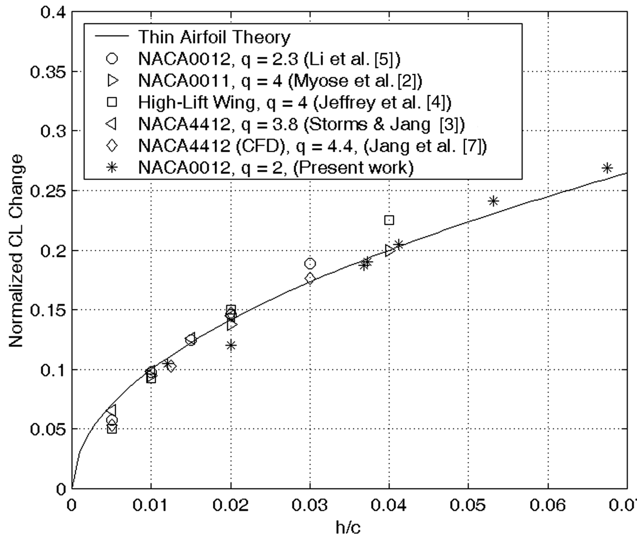

Fig. 4 Normalized lift coefficient enhancement as a function of normalized Gurney flap height.

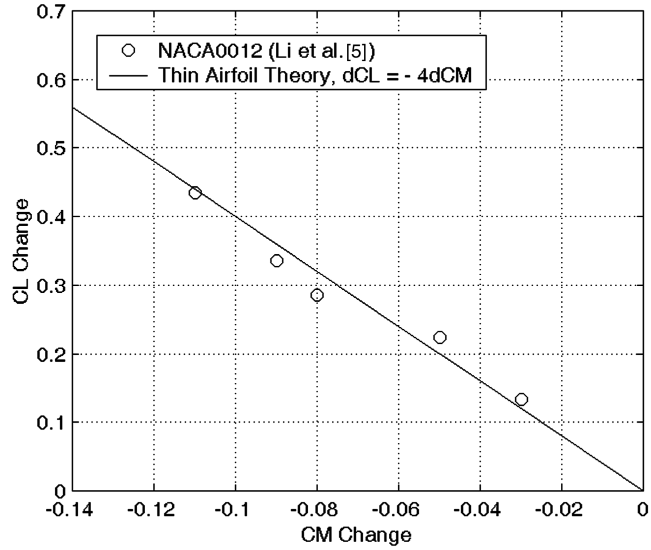

Fig. 6 Lift coefficient change vs pitching moment coefficient change.

height can be lucidly illustrated. It is complementary to experimental and computational studies.

Comparison with Measurements and Calculations

Figure 4 compares the normalized lift enhancement $\Delta C_l/q = \sqrt{h/c}$ with the experimental and CFD results, where the factor q depending on the model geometry and test conditions is adjusted to fit the results obtained in different measurements and numerical calculations. These data are collapsed into a single square-root function of h/c as predicted by Eq. (27). Three sets of data for the symmetrical main airfoils (NACA0011 and NACA0012) [2,5] are used, whereas others are used for the cambered main airfoils [3,4,7]. To provide additional data, particularly for higher Gurney flaps, we conducted Gurney flap measurements for the chord Reynolds number 6×10^5 in the Advanced Design Wind Tunnel of Western Michigan University. The main wing was a ceramic NACA0012 airfoil section and a six-component internal force balance was used to measure the aerodynamic forces. The Gurney flap height ranged from 1.2 to 6.75%c. The chord and span of the model are 10 and 12 in., respectively. Two finite end plates (18 × 13 in.) were attached at the wing section tips, serving the support for the model and reducing the three-dimensionality of flow. Because the end plates were finite, strong tip vortices were still observed even though they were modified by the end plates. The effective aspect ratio is 4.42 due to the effect of the finite end plates, which is determined by fitting the measured lift slope based on McCormick's formula [16]. The data obtained in the experiments are plotted in Fig. 4. Besides the experimental data, the CFD results of Jang et al. [7] are also used for comparison. Although the present analysis is for a Gurney flap mounted on a symmetrical main airfoil, Eqs. (27) and (28) are applicable to cambered main airfoils as the first-order approximation. Figure 5 shows a comparison between Eq. (28) and measurements [5] for the change of the pitching moment coefficient. Interestingly, the experimental results for wings with different aspect ratios follow the square-root laws, Eqs. (27) and (28), which are obtained in a strictly two-dimensional case. It is indicated that the three-dimensional effect is mainly contained in the proportional coefficient. To examine the theoretical estimate $\Delta C_l/\Delta C_{m,c/4} \approx -4$, ΔC_l is plotted as a function of $\Delta C_{m,c/4}$ in Fig. 6 for a NACA0012 airfoil [5]. The theoretical relation is in good agreement with the experimental data, which is of particular interest because it does not contain any free parameter in the initial approximation.

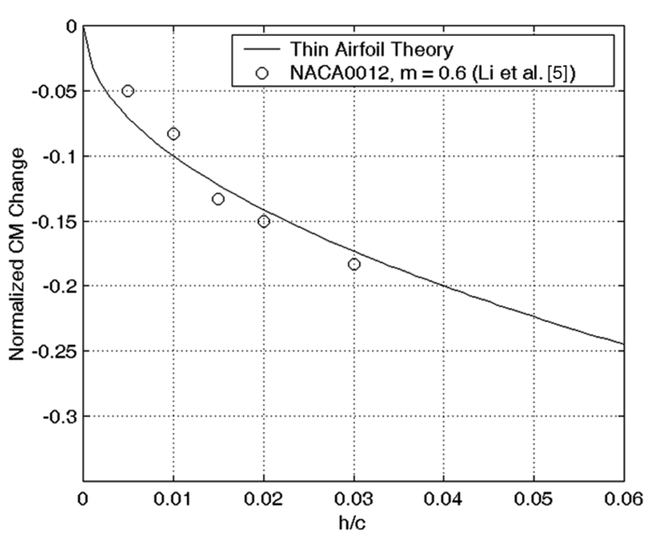

Fig. 5 Normalized pitching moment coefficient change as function of normalized Gurney flap height.

Conclusions

Flow over an airfoil with a Gurney flap is aerodynamically modeled by a main vortex-sheet segment connected with a deflected short vortex-sheet segment in the framework of thin-airfoil theory. Because the effective hydrodynamic deflection by a Gurney flap is locally large, the generalized formulation of thin-airfoil theory is developed for Gurney flaps. A solution of the generalized thin-airfoil integral equation for the vortex strength is obtained by the method of successive approximations. Both the lift and pitching moment coefficient increments are proportional to the square root of the normalized Gurney flap height. Therefore, a ratio between the lift coefficient and pitching moment increments is a constant independent of the flap height. The theoretical relations are in good agreement with the experimental and numerical data. The Gurney flap lift enhancement is interpreted as a special camber effect.

Acknowledgments

This work was supported by the Air Force Office of Scientific Research, United States Air Force, under the grant number FA9550-06-1-0187.

References

[1] Liebeck, R. H., "Design of Subsonic Airfoils for High Lift," *Journal of Aircraft*, Vol. 15, No. 9, 1978, pp. 547–561.
[2] Myose, R., Papadakis, M., and Heron, I., "Gurney Flap Experiments on Airfoils, Wings, and Reflection Plane Model," *Journal of Aircraft*, Vol. 35, No. 2, 1998, pp. 206–211.

[3] Storms, B., and Jang, C. S., "Lift Enhancement of an Airfoil Using a Gurney Flap and Vortex Generators," *Journal of Aircraft*, Vol. 31, No. 3, 1994, pp. 542–547.
[4] Jeffrey, D., Zhang, X., and Hurst, D. W., "Aerodynamics of Gurney Flaps on a Single-Element High-Lift Wing," *Journal of Aircraft*, Vol. 37, No. 2, 2000, pp. 295–301.
[5] Li, Y., Wang, J., and Zhang, P., "Effects of Gurney Flaps on a NACA0012 Airfoil," *Flow, Turbulence and Combustion*, Vol. 68, No. 1, 2002, pp. 27–39.
[6] Li, Y., Wang, J., and Zhang, P., "Influences of Mounting Angles and Locations on the Effects of Gurney Flaps," *Journal of Aircraft*, Vol. 40, No. 3, 2003, pp. 494–498.
[7] Jang, C. S., Ross, J. C., and Cummings, R. M., "Numerical Investigation of an Airfoil with a Gurney Flap," *Aircraft Design*, Vol. 1, No. 2, 1998, pp. 75–88.
[8] Ross, J., Storms, B. L., and Carrannanto, P. G., "Lift-Enhancing Tabs on Multielement Airfoils," *Journal of Aircraft*, Vol. 32, No. 3, 1995, pp. 649–655.
[9] Meyer, R., Hage, W., Bechert, D. W., Schatz, M., and Thiele, F., "Drag Reduction on Gurney Flaps by Three-Dimensional Modification," *Journal of Aircraft*, Vol. 43, No. 1, 2006, pp. 132–140.
[10] Gai, S. L., and Palfrey, R., "Influence of Trailing-Edge Flow Control on Airfoil Performance," *Journal of Aircraft*, Vol. 40, No. 2, 2003, pp. 332–337.
[11] Glauert, H., *Elements of Aerofoil and Airscrew Theory*, 2nd ed., Cambridge Univ. Press, Cambridge, England, 1993, Chap. 7.
[12] Anderson, J. D., *Fundamentals of Aerodynamics*, 2nd ed., McGraw–Hill, New York, 1984, Chap. 4.
[13] Brandao, M. P., "Improper Integrals in Theoretical Aerodynamics: The Problem Revisited," *AIAA Journal*, Vol. 25, No. 9, 1987, pp. 1258–1260.
[14] Katz, J., and Plotkin, A., *Low-Speed Aerodynamics*, 2nd ed., Cambridge Univ. Press, Cambridge, England, 2001, pp. 113–114.
[15] von Mises, R., *Theory of Flight*, Dover, New York, 1959, p. 269.
[16] McCormick, B. W., *Aerodynamics, Aeronautics and Flight Mechanics*, 2nd ed., Wiley, New York, 1995, p. 116.